

Circuit Theoretic Considerations of LED Driving: Voltage-Source Versus Current-Source Driving

Zheng Dong, Chi K. Tse, *Fellow, IEEE*, and S. Y. Ron Hui, *Fellow, IEEE*

Abstract—Light-emitting-diodes (LEDs) are solid-state devices with specific v - i characteristics. In this paper we study the basic requirement of the driving circuits and discuss the proper approach to driving LEDs in view of their characteristics. We compare voltage source driving and current source driving, and discuss their relative advantages and constraints. We specifically introduce the use of duality principle for developing new current-source drivers which are less known but are theoretically more versatile compared to their conventional voltage-source counterparts. The study highlights the effects of the choice of circuit topologies on current and voltage ripples, duty cycle variation, sensitivity, and nonlinearity of LED drivers. This paper presents a systematic and comparative exposition of the circuit theory of driving LEDs, with experimental evidences supporting the major conclusions. Given various forms of input sources and output load characteristics, we generate possible circuit configurations that are suitable for driving LEDs. We illustrate how a basic two-stage power supply can lead to an effective LED driver design. Finally, the experiments have been built and tested to validate the theoretical results.

Index Terms—Voltage source converters, current source converters, LED driver, design environment, two-stage power supply.

I. INTRODUCTION

SOLID-STATE loads have become increasingly popular in residential, commercial and business environment, e.g., light-emitting-diode (LED) lighting systems [1]–[5]. According to the statistics, about 19% of global electricity is consumed by lighting [6]. The LED has become a promising new generation light source because of the advantages of environmental safety, long life expectancy and high efficiency [7]. A trend of replacing traditional lightings by LEDs is formed. Renewable energy sources have also been used in modern microgrid power distribution systems [8]. For photovoltaic devices [9], superconductive magnetic energy storages [10] and some specific applications [11], we regard the output or load side as current sources. The recent trend in the use of solid-state loads and renewable sources has created new challenges in power management system design, especially in the design of power conversion systems which have traditionally been dominated by voltage sources and resistive loads.

Manuscript received March 1, 2017. This work is supported by Hong Kong Research Grants Council under Theme-Based Research Project No. T22-715/12-N.

Z. Dong and C.K. Tse are with the Department of Electronic and Information Engineering, Hong Kong Polytechnic University, Hong Kong. (Email: z.dong@connect.polyu.hk, encktse@polyu.edu.hk)

S.Y.R. Hui is with the Department of Electrical and Electronic Engineering, The University of Hong Kong, Hong Kong. (Email: ronhui@eee.hku.hk)

Digital Object Identifier XXXXXXXXXXXXXXXXXXXX.

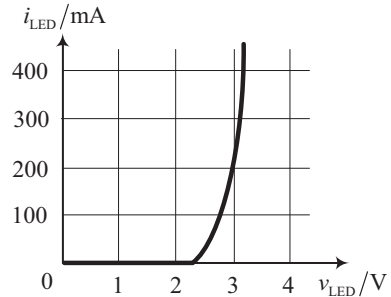


Fig. 1. Typical LED's v - i characteristic.

Traditional power converters, e.g., buck and boost converters [12]–[19], are designed for input voltage sources that are assumed for most everyday applications. Basically, for a voltage-source (VS) converter, the input voltage is fixed, and the output of the converter can be regarded as a *voltage source* controlled through the duty cycle, i.e.,

$$V_o = F(D)V_{in} \quad (1)$$

where D is the duty cycle and $F(\cdot)$ is the function defining the input-to-output voltage transfer ratio. In theory, when a VS converter is used to drive an LED, the output current level has to be controlled by varying the output voltage which is adjusted via the duty cycle.

A typical LED's v - i characteristic is shown in Fig. 1. The voltage of the LED basically varies in a rather narrow range with the change of the current of the LED. The LED can thus be regarded as an approximate voltage source.

Taking the crude view of an LED as a voltage source, the use of a VS converter and a current-source (CS) converter driving the LED is illustrated in Fig. 2(a). From a circuit theoretic viewpoint [20], it is fundamentally undesirable when voltage sources are connected in a loop. When the load is a voltage source, such as an LED, the driver should deliver controllable current to the load, as shown in Fig. 2(b). So it is fundamentally more desirable to construct a current source to drive an LED.

Through the use of duality principle [20], a family of current-source (CS) converters can be readily obtained from the most known VS converters. In a dual fashion, the output current of a CS converter can be obtained by controlling the duty cycle given a fixed input current, i.e.,

$$I_o = F'(D)I_{in} \quad (2)$$

where D is again the duty cycle and $F'(\cdot)$ is the function defining the input-to-output current transfer ratio. The output

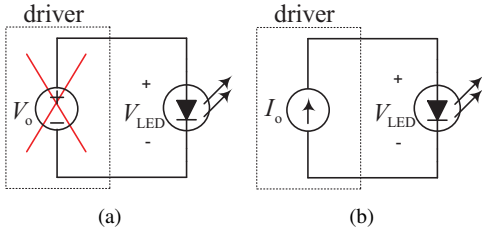


Fig. 2. Basic considerations. (a) Voltage sources in parallel; (b) voltage source connects current source.

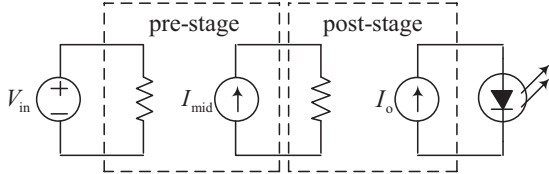


Fig. 3. Two-stage power supply.

can then be regarded as a controllable current source which is suitable to drive an LED. Despite their long history of existence [21], CS converters are still relatively less analyzed or applied for driving LEDs. The main reason for this omission is that voltage sources are a more common form of power source and can be connected to the input termination of a VS converter directly. Furthermore, resistive loads are also a commonly assumed form of loads and more widely included in analysis. A comparatively smaller amount of literature has thus been devoted to discuss the application of CS converters for driving LEDs [22]–[25].

There are two basic dimming methods for LEDs, namely, pulse-width modulation (PWM) dimming and analog dimming [26]. The PWM dimming method is realized by switching on and off an LED string repeatedly while the LED's current is kept constant. However, if the frequency of the LED string's switch is not chosen appropriately, flickering and stroboscopic phenomena would occur [27]. Analog dimming is done by regulating the value of the forward current that flows into the LED. It can avoid the flickering and stroboscopic effect. Based on the considerably wide linear relationship between the current and the luminance of the LED, in this paper, we compare the analog dimming method applied to VS and CS converters.

For most practical purposes, the input of an LED driver is required to connect to a voltage source which is still the most common form of power source. Moreover, a voltage source cannot be connected directly with the input port of a CS converter, leading to obvious constraints in practical applications. The focus of the analysis will thus be on the circuit requirement for converting power from a voltage input termination to an LED output termination. In order to fully utilize a CS converter to construct a controllable current source, we present a two-stage power supply as a basic solution. A front-stage provides a constant current source, the post-stage delivers current to the LED. This forms the basic guiding principle for design, as shown in Fig. 3.

This paper is organized as follows. Section II reviews the

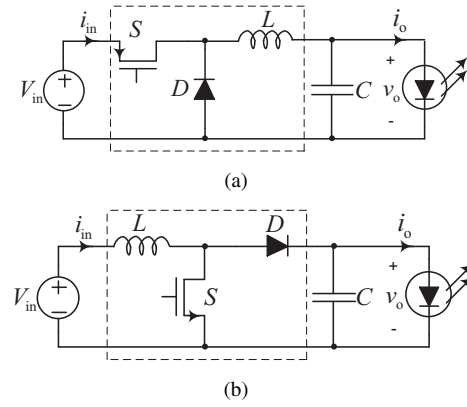


Fig. 4. Conventional voltage-source (VS) converters. (a) Buck and (b) boost converter.

duality principle and examines the circuit transformation of power conversion circuits via duality principle. Section III compares the VS and CS converters. This section investigates VS and CS drivers in terms of the output ripple amplitude, the range of duty cycle variation, the sensitivity of the output current to the change of duty cycle, and the nonlinearity of the control relation. In Section IV, based on a two-stage power supply structure, we present several driver circuits based on CS converters which are suitable candidates for driving LEDs. We study the specific configuration of a VS buck converter cascading with a CS buck converter, and analyze its operating principle, the range of the input voltage and the relationship between the intermediate current and the duty cycle. We emphasize that proper application of circuit concepts would form the basis of design of effective driving circuits for LED applications. Some practical configurations of 10-W LED driving circuits are presented in Section V for the purpose of illustration. Finally, Section VI concludes the paper.

II. CIRCUIT DUALITY PRINCIPLE

The conventional voltage-source buck and boost converters are shown in Figs. 4. The input termination is fed by a voltage source, which is normally a constant DC voltage. The converters deliver voltage to an LED load, and the duty cycle controls the input-to-output voltage ratio. Thus, the output can be regarded as a controllable voltage source.

For a VS converter, applying volt-time balance, the steady-state voltage gain, M , is determined as:

$$M = \frac{V_o}{V_{in}} = \begin{cases} D & \text{VS buck converter} \\ \frac{1}{1-D} & \text{VS boost converter} \end{cases} \quad (3)$$

where D is the steady-state duty cycle, V_{in} and V_o are input and output voltages.

The duality transformation of a VS converter to a CS converter follows the following standard procedure [20]:

- 1) A dual graph is obtained, as illustrated in Fig. 5.
- 2) Voltage sources are replaced by current sources, and vice versa. Capacitors are replaced by inductors, and vice versa. Resistors (R) are replaced by conductors ($G = 1/R$).

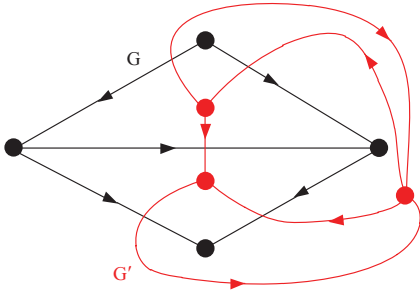


Fig. 5. Graph G and its dual G' .

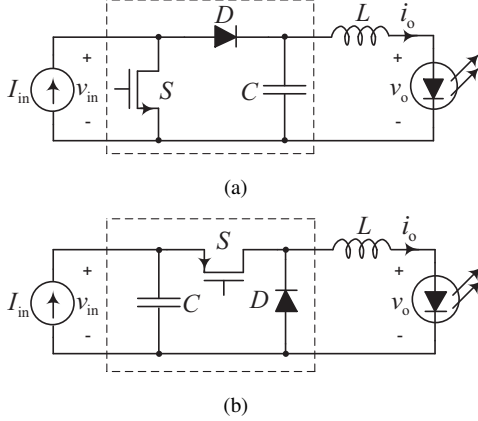


Fig. 6. Current-source (CS) converters. (a) CS buck converter; (b) CS boost converter.

- 3) An “on” switch is replaced an “off” switch, and vice versa. Hence, duty cycle D becomes $(1 - D)$.

The current-source counterparts of the buck and boost converters are shown in Fig. 6. The input termination is fed by a current source. The converters deliver current to an LED load. The duty cycle controls the current ratio of the input and output. Thus, the output can be regarded as a controllable current source.

For a CS converter, the steady-state current gain, M' , is directly obtained by replacing D with $1 - D$ in the corresponding VS equation, i.e.,

$$M' = \frac{I_o}{I_{in}} = \begin{cases} 1 - D & \text{CS buck converter} \\ \frac{1}{D} & \text{CS boost converter} \end{cases} \quad (4)$$

where I_{in} and I_o are input and output currents.

There are two variables of an LED, i.e., the forward voltage and the operating current. According to (3), for a VS converter, we can adjust the duty cycle to control the output voltage which is connected to the forward voltage of the LED. The operating current, which determines the luminance, changes with the forward voltage. Moreover, according to (4), for a CS converter, we can theoretically adjust the duty cycle to control the operating current of the LED, leading to direct luminance control.

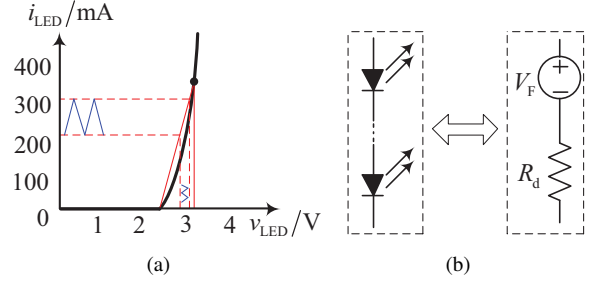


Fig. 7. Ripple analysis from linearized model. (a) LED's voltage ripple vs. current ripple; (b) LED's simplified model.

TABLE I
PARAMETERS OF TEST CIRCUITS

	VS buck conv.	CS buck conv.	VS boost conv.	CS boost conv.
V_{in}	48 V	—	24 V	—
I_{in}	—	500 mA	—	100 mA
T	20 μ s	20 μ s	20 μ s	20 μ s
L	2000 μ H	2000 μ H	2000 μ H	2000 μ H
C	47 μ F	47 μ F	47 μ F	47 μ F

III. COMPARISON OF VOLTAGE-SOURCE AND CURRENT-SOURCE DRIVERS

In reality, the LED is a non-ideal voltage source having a characteristic v - i relationship, as typically shown in Fig. 7(a). When the forward voltage is higher than its cut-in voltage V_F , the LED's current is changing in an approximately linear manner with the LED's voltage. Therefore, we may derive a simplified model as shown in Fig. 7(b). The ratio of $\Delta v_o / \Delta i_o$ for a specific LED can be empirically found as

$$\frac{\Delta v_o}{\Delta i_o} = R_d = \frac{3.15 - 2.27 \text{ V}}{350 \text{ mA}} = 2.5 \Omega \quad (5)$$

Here, we compare the VS and CS based drivers in terms of the output ripple amplitude, the range of duty cycle variation, the sensitivity of output current to change of duty cycle, and the extent of nonlinearity. The load is composed of a string of n white LEDs stacked in series. All converters are designed to operate in continuous conduction mode. For effective illustration, we present alongside the following analysis a set of measured data from experimental circuits. The circuit parameters of the prototypes are listed in Table I. Each LED is rated at 1 W and 350 mA. All converters employ the same set of components: MOSFET, diode, inductor and capacitor. In the test circuits, we set $n = 10$.

A. Output Ripples

In the case of the VS buck converter, the current ripple of the inductor can be obtained as

$$\Delta i_L = \frac{V_{in} - (V_F + I_o R_d)}{L} DT \quad (6)$$

where I_o is the steady-state average output (load) current, V_F and R_d are as defined in Fig. 7. The output voltage

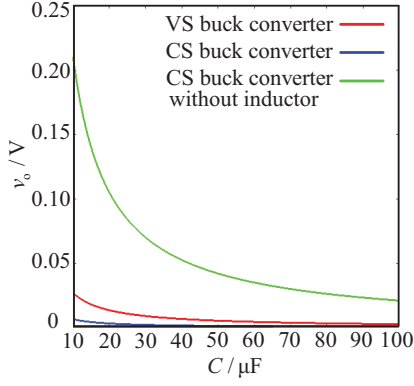


Fig. 8. Relationship between ripple and capacitance value of VS and CS buck converters

ripple, which corresponds to the current ripple in (6), can be calculated as

$$\Delta v_o = \frac{\{V_{in} - n(V_F + I_o R_d)\} DT^2}{8LC} \quad (7)$$

In the case of the CS buck converter, the current ripple of the inductor, which is also the output current ripple, can be calculated as

$$\Delta i_o = \frac{(I_{in} - I_o)(1 - D)T^2}{8LC} \quad (8)$$

where I_o is the steady-state average output current. According to (5) and (8), the equivalent voltage ripple of the CS buck converter is

$$\Delta v_o = \frac{nR_d(I_{in} - I_o)(1 - D)T^2}{8LC} \quad (9)$$

Furthermore, in the case of the CS buck converter, if inductor L is removed, the new output voltage ripple of the CS buck converter can meet the usual requirement as long as the capacitance value is chosen appropriately. The output voltage ripple of the CS buck converter without the inductor is

$$\Delta v_o = \frac{I_{in} - I_o}{C} (1 - D)T \quad (10)$$

Taking $I_o = 350$ mA as an example, according to equations (7), (9) and (10), the voltage ripples of the LEDs for different drivers are plotted in Fig. 8, from which we see that the voltage (or current) ripple magnitude of the LED driven by the CS buck converter is smaller than that driven by the VS buck converter having the same L and C values (same size). Furthermore, the output voltage (or current) ripple of the CS buck converter without the inductor increases slightly. However, with a slightly larger capacitance, the ripple can be dramatically reduced to meet the requirement. Without the inductor, the size, weight and cost of the circuit can be significantly reduced, as shown in Fig. 9.

In the case of the traditional VS boost converter, the output voltage ripple is

$$\Delta v_o = \frac{I_o DT}{C} \quad (11)$$

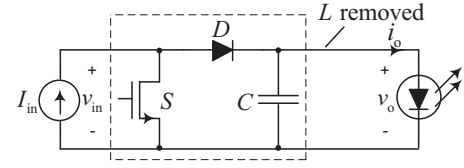


Fig. 9. Current-source (CS) buck converter with output inductor removed

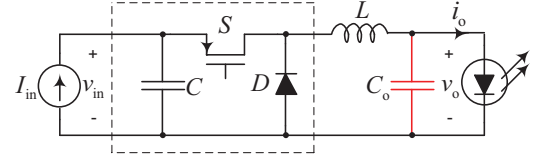


Fig. 10. Current-source (CS) boost converter with additional output capacitor

where I_o is the steady-state average output (load) current, and the current ripple in an LED load driven by the VS boost converter is

$$\Delta i_o = \frac{I_o DT}{nR_d C} \quad (12)$$

In the case of the CS boost converter, the current ripple of the inductor is also the output current ripple, which can be found as

$$\Delta i_o = \Delta i_L = \frac{n(V_F + I_o R_d)}{L} (1 - D)T \quad (13)$$

Since the LED's current is the inductor's current, the current ripple amplitude in the CS boost driving converter is larger than that in the VS boost converter. It should be noted that for the CS boost converter, in order to reduce the output current ripple, a capacitor should be connected to the output terminal, as shown in Fig. 10.

The current ripple of the LED driver using a CS boost converter connected with an additional capacitor is given by

$$\Delta i_o = \frac{(V_F + I_o R_d)(1 - D)T^2}{8nR_d L C_o} \quad (14)$$

Taking $I_o = 350$ mA as an example, according to (12), (13) and (14), the current ripples of the LEDs using different drivers are plotted in Fig. 11. Here, we see that the current ripple amplitude of the CS boost converter is much larger than in the other drivers. After inserting an extra capacitor, the current ripple can be reduced significantly. However, the size, weight and cost of the circuit will be inevitably increased.

B. Range of Duty Cycle Variation

For the VS converters, the input voltage is the constant voltage source. Based on (3), we can derive the driver's transfer characteristics for VS buck and VS boost converters. Combining the converter's transfer characteristic and the LED's v - i characteristic, we obtain an overall transfer characteristic as shown in Fig. 12(a). For the CS converters, however, the input current is constant. Based on (4) and the LED's v - i characteristic, we obtain the overall transfer characteristic as shown in Fig. 12(b).

From Fig. 12(a), it is obvious that, for VS driving, the output current can be changed by adjusting the output voltage,

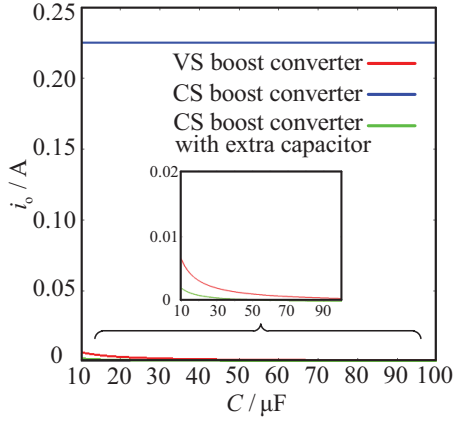


Fig. 11. Relationship between ripple and the capacitance value of VS and CS boost converters

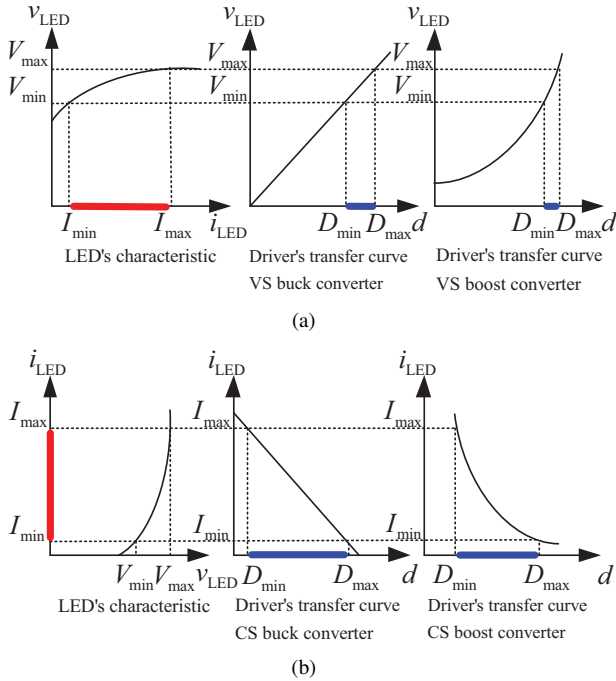


Fig. 12. Current control under VS and CS driving. (a) Variations of LED current and voltage under VS driving; (b) variations of LED current and voltage under CS driving.

which can be adjusted or controlled via the duty cycle over a rather narrow range, making the control rather sensitive. For CS driving, however, as shown in Fig. 12(b), the output current can be changed by adjusting the duty cycle directly. Thus, the corresponding change in the duty cycle is much greater, and the current control can be achieved with the duty cycle varying over a wide range. Suppose the range of duty cycle is the value of duty cycle from D_{\min} to D_{\max} , i.e.,

$$D_{\text{span}} = D_{\max} - D_{\min} \quad (15)$$

Based on the simplified model of Fig. 7, the theoretical duty cycle ranges of these converters are shown in Table II. In general, CS converters have a wider range of duty cycle variation than VS converters over the same range of

current variation. Thus, CS converters are more desirable for applications requiring higher output current resolution.

TABLE II
THEORETICAL DUTY CYCLE RANGE ($I_o = 150\text{--}350$ mA)

	VS buck	CS buck	VS boost	CS boost
D_{\max}	0.656	0.700	0.238	0.667
D_{\min}	0.552	0.300	0.094	0.286
D_{span}	0.104	0.400	0.144	0.381

C. Sensitivity

We define *sensitivity* as the absolute ratio of the variation of the steady-state output current (ΔI_o) to the corresponding variation of the steady-state duty cycle (ΔD). Thus, *sensitivity* is a function of D and can be written as:

$$S = |f(D)| = \left| \frac{d\Delta I_o}{d\Delta D} \right| \quad (16)$$

Based on the simplified model of LED, and using (3), (4) and (5), the relationship between I_o and D for VS and CS converters is

$$I_o = \begin{cases} \frac{V_{\text{in}}D}{nR_d} - \frac{V_F}{R_d} & \text{VS buck converter} \\ I_{\text{in}}(1-D) & \text{CS buck converter} \\ \frac{V_{\text{in}}}{nR_d(1-D)} - \frac{V_F}{R_d} & \text{VS boost converter} \\ \frac{I_{\text{in}}}{D} & \text{CS boost converter} \end{cases} \quad (17)$$

According to (16) and (17), the expression of *sensitivity* can be given as

$$S = \begin{cases} \frac{V_{\text{in}}}{nR_d} & \text{VS buck converter} \\ I_{\text{in}} & \text{CS buck converter} \\ \frac{V_{\text{in}}}{nR_d(1-D)^2} & \text{VS boost converter} \\ \frac{I_{\text{in}}}{D^2} & \text{CS boost converter} \end{cases} \quad (18)$$

The maximal/minimal value of the *sensitivity* is the worst/best value of S , i.e.,

$$\begin{cases} S_{\max} = \left| \frac{d\Delta I_o}{d\Delta D} \right|_{\max} \\ S_{\min} = \left| \frac{d\Delta I_o}{d\Delta D} \right|_{\min} \end{cases} \quad (19)$$

where $(\Delta I_o)_{\max}$ and $(\Delta I_o)_{\min}$ are the maximal and minimal ΔI_o corresponding to the variation of duty cycle ΔD . In practice, a smaller S is more desirable because of the smaller ΔI_o caused by the same variation of D . Table III and Fig. 13 show the variation in S . According to Fig. 13, CS converters have smaller *sensitivity* than VS converters for the whole range of duty cycle.

TABLE III
THEORETICAL SENSITIVITY ($I_o = 150\text{--}350\text{ mA}$)

	VS buck	CS buck	VS boost	CS boost
S_{\max}	1.92	0.50	1.65	1.22
S_{\min}	1.92	0.50	1.17	0.22

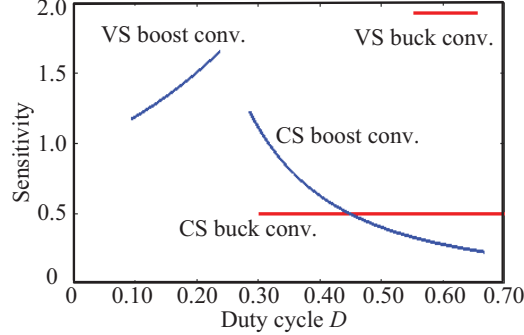


Fig. 13. Sensitivity S versus duty cycle D .

D. Nonlinearity

According to equation (17), we can plot the duty-cycle-to-output transfer characteristic of the drivers, as shown in Fig. 14. In order to evaluate the linearity of the transfer characteristic, we adopt a measure, known as *nonlinearity* N [28] which is defined as

$$N = \frac{\Delta W}{W} \quad (20)$$

where W is the root-mean-square of the transfer characteristic $I_o = f(D)$ in equation (17), ΔW is the root-mean-square of the difference between the transfer characteristic of (17) and the line $I_o = f_L(D)$ that connects the border points. Specifically we have

$$\begin{cases} W = \sqrt{\frac{\int_{D_{\min}}^{D_{\max}} f^2(D) dD}{D_{\max} - D_{\min}}} \\ \Delta W = \sqrt{\frac{\int_{D_{\min}}^{D_{\max}} [f(D) - f_L(D)]^2 dD}{D_{\max} - D_{\min}}} \end{cases} \quad (21)$$

Theoretical values of nonlinearity N are calculated and given in Table IV, based on the simplified model of LED shown in Fig. 7.

The nonlinearity can affect the stability of the control system. In general, a smaller N is more desirable. According to Fig. 14 and Table IV, the VS and CS buck converters have smaller values of N than the VS and CS boost converters.

IV. TWO-STAGE DESIGN OF LED DRIVERS

From the foregoing analysis above, we see that the CS converters have obvious advantages when applied to drive LEDs from the circuit theoretic viewpoint. However, current sources are not normally available as power sources in most practical environment. Instead, voltage source is the default form of power source though it cannot be connected directly to the input port of a CS converter. It is thus necessary to

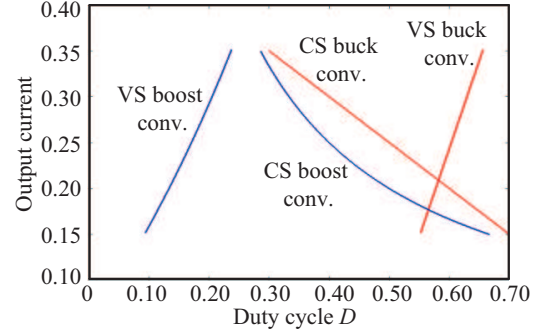


Fig. 14. Output current I_o versus duty cycle D .

TABLE IV
THEORETICAL NONLINEARITY ($I_o = 150\text{--}350\text{ mA}$)

	VS buck	CS buck	VS boost	CS boost
W	0.2583	0.2566	0.2528	0.2291
ΔW	0	0	0.0044	0.0303
N	0	0	0.0174	0.1323

introduce a pre-stage that feeds current to the CS converter stage, as presented in Fig. 15, which is based on the design principle shown in Fig. 3. The input to the pre-stage is a voltage source, and the output is a constant current source feeding a post-stage which drives an LED load. Thus, this two-stage configuration consists of a VS converter interfacing the voltage input and a CS converter delivering controllable current to an LED load.

The exact circuit configuration would depend on the specific choice of the converter circuits. When the pre-stage is a VS buck converter, the current of inductor L_1 in Fig. 15 can be controlled to stay constant without using L_{mid} and C_{mid} . When the pre-stage is a VS boost converter, however, the use of L_{mid} and C_{mid} is mandatory in order to deliver a controllable current to the load. Furthermore, when the post-stage is a CS buck converter, inductor L_o connected with the output port can be removed, as explained previously in Section III-A. Also, when the post-stage is a CS boost converter, an extra parallel capacitor is needed at the output, as explained in Section III-A.

From the foregoing discussion, the simplest structure contains a VS buck converter as the pre-stage and a CS buck converter as the post-stage, as shown in Fig. 16 with L_{mid} , C_{mid} , and L_o all eliminated. It should be noted that a constant current is maintained in i_{L1} to feed the post-stage CS converter, and that a NOT gate is inserted for the necessary signal inversion as required by the dual switching operation of the CS converter. For the two-stage design consisting of a VS buck converter cascading a CS buck converter, there are three operating modes in each switching cycle, as illustrated in Fig. 17.

When $D_1 + D_2 < 1$, the circuit operates with three switching stages or modes, as depicted in Figs. 17(a), 17(b) and 17(d). When S_1 is on and S_2 is off, $V_{\text{in}} - V_o$ charges the inductor, and i_{L1} ramps up. When S_1 is off and S_2 is off, V_o discharges the inductor, and i_{L1} ramps down while supplying current to

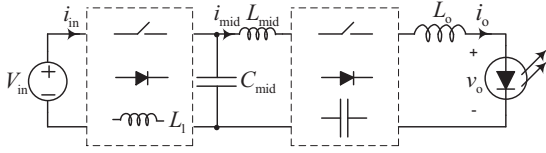


Fig. 15. Two-stage design for LED driver.

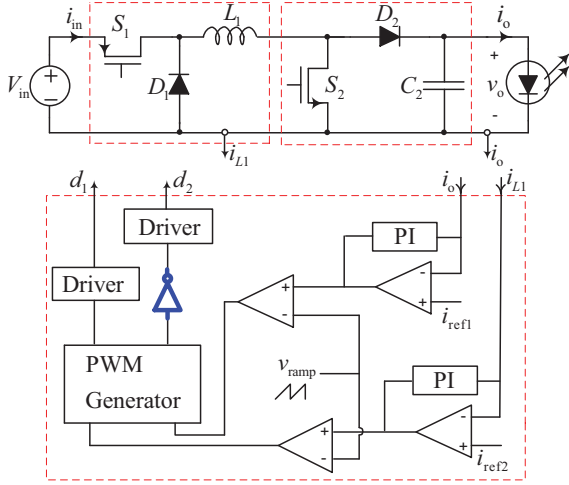


Fig. 16. Simplest two-stage design consisting of a VS buck converter cascading a CS buck converter.

the load. When S_1 is off, S_2 is on, the inductor's current is in the freewheeling mode, the capacitor is discharged to the load. The key waveforms are shown in Fig. 18(a).

When $D_1 + D_2 < 1$, another set of three switching stages is assumed, as shown in Figs. 17(a), 17(c) and 17(d). When S_1 is on and S_2 is off, $V_{in} - V_o$ discharges the inductor, and i_{L1} ramps down. When S_1 is on and S_2 is on, V_{in} charges the inductor, and i_{L1} ramps up, and the capacitor is discharged to the load. When S_1 is off and S_2 is on, the inductor current is in a freewheeling mode, with the capacitor delivering current to the load. The key waveforms are shown in Fig. 18(b).

For the case of $D_1 + D_2 < 1$, according to the volt-time balance of the inductor, we get

$$(V_{in} - V_o)D_1 = V_o(1 - D_1 - D_2) \quad (22)$$

The voltage conversion ratio of the circuit is given by

$$V_{in} = \frac{(1 - D_2)}{D_1} V_o \quad (23)$$

Since $D_1 < 1 - D_2$, the range of the input voltage in this case is

$$V_{in} > V_o \quad (24)$$

Likewise, for $D_1 + D_2 > 1$, according to the volt-time balance of the inductor, we get

$$(V_o - V_{in})(1 - D_2) = V_{in}(D_1 + D_2 - 1) \quad (25)$$

Using (4) and (25), D_1 and D_2 can be obtained as

$$\begin{cases} D_1 = \frac{V_o I_o}{V_{in} I_{L1}} \\ D_2 = 1 - \frac{I_o}{I_{L1}} \end{cases} \quad (26)$$

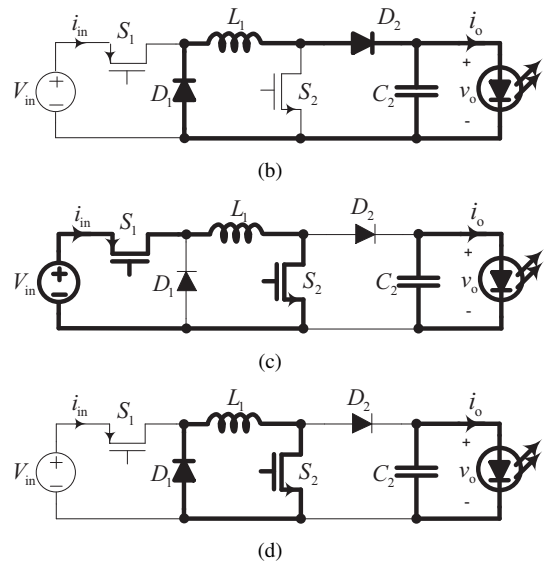
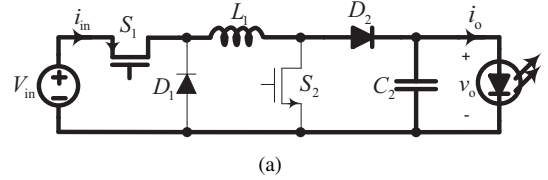


Fig. 17. Operating modes. (a) S_1 is on and S_2 is off; (b) S_2 is off and S_2 is off; (c) S_1 is on and S_2 is on; (d) S_1 is off and S_2 is on.

Since $D_1 > 1 - D_2$ and $D_1 < 1$, the range of the input voltage in this case is:

$$\frac{V_o I_o}{I_{L1}} < V_{in} < V_o \quad (27)$$

Combining the two cases, the entire range of the input voltage is

$$V_{in} > \frac{V_o I_o}{I_{L1}} \quad (28)$$

A graphical representation of the input voltage range is shown in Fig. 19.

Using (26), when I_o and V_o are fixed, we can derive the relationship between I_o , D_1 and D_2 , as shown in Fig. 20. As I_{L1} approaches I_o , the transfer characteristics in Fig. 20 will move from the blue line toward the red, broadening the range of the duty cycles and thus improving the sensitivity of the control. However, from Fig. 19, as I_{L1} approaches I_o , the minimum input voltage V_{in-min} will increase and the input voltage range will be limited. For this circuit, both step-down and step-up function can be achieved. However, in choosing the value of I_{L1} , the range of the duty cycle and the range of the input voltage are conflicting factors. Getting a wider range of the duty cycle means narrowing the range of the input voltage, and vice versa. Thus, as usual in engineering design, an optimal choice should be made to balance the conflicting factors according to the application under consideration.

In practice, if transformer isolation is desired, flexibility exists in combining the two stages through appropriate switching arrangement and transformer design. An example of a dual power supply with power factor correction and current load driving can be found in [29], which represents an early attempt

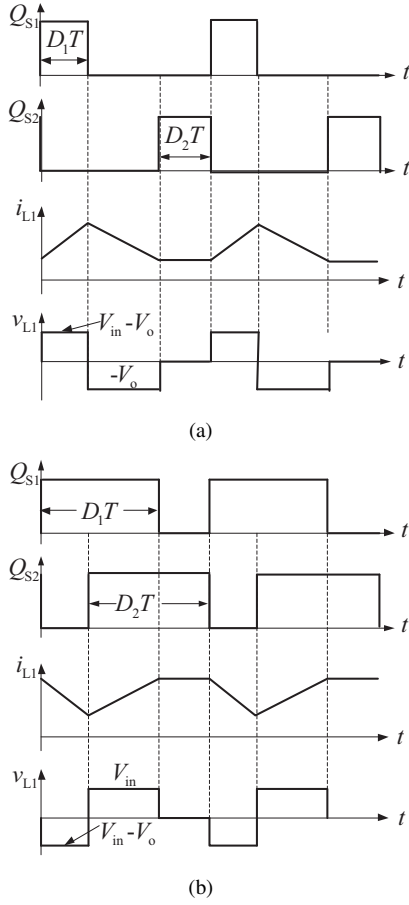


Fig. 18. The current waveforms. (a) Current waveform under $D_1 + D_2 < 1$; (b) Current waveform under $D_1 + D_2 > 1$.

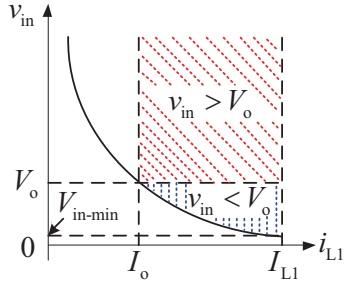


Fig. 19. Range of input voltage.

in applying duality principle for deriving alternative current-based topologies. It should be noted that although the design described in [29] did not explicitly address the LED driving applications at the time it was published, it should now become apparent that such a design is highly relevant to the driving of LED lighting systems.

V. EXPERIMENTAL RESULTS

In order to show the feasibility of the VS and CS converters and to validate the theoretical analysis, laboratory prototypes were built with parameters and components given in Table I.

Experimental waveforms for the output ripples are shown in Fig. 21. The voltage ripples of LEDs driven by the VS buck

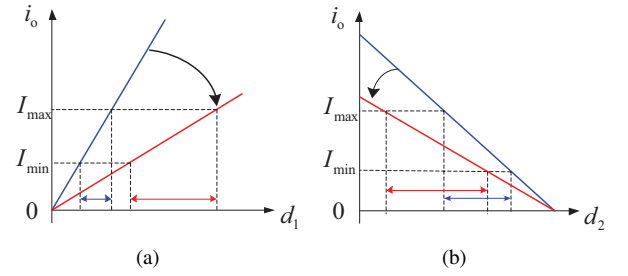


Fig. 20. Output current I_o versus (a) D_1 and (b) D_2 .

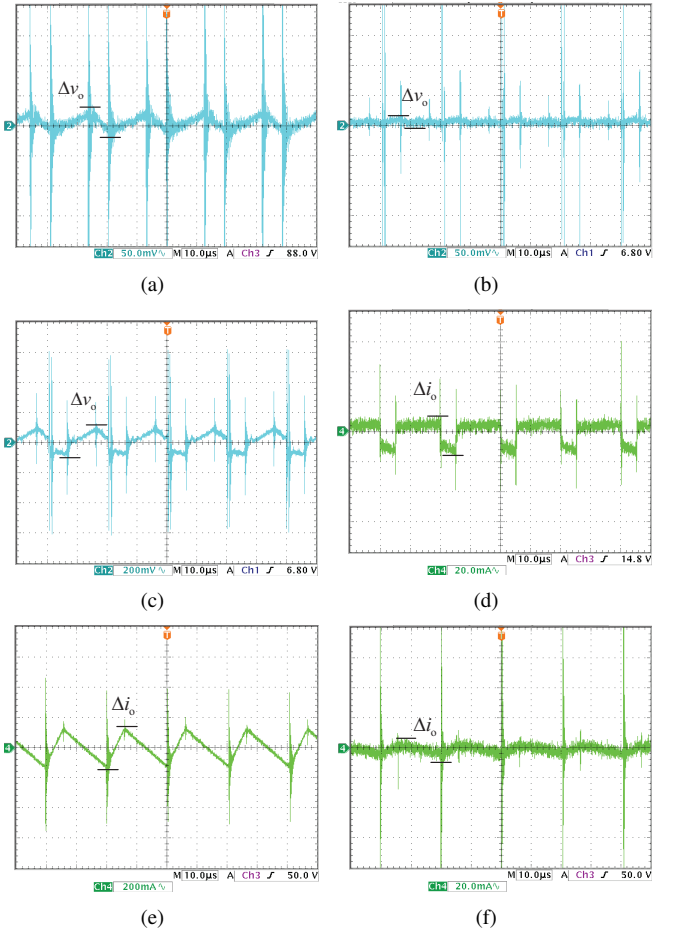


Fig. 21. LED's output ripples. (a) VS buck converter; (b) CS buck converter; (c) CS buck converter without inductor; (d) VS boost converter; (e) CS boost converter; (f) CS boost converter with extra capacitor

converter, CS buck converter and CS buck converter without the inductor are 50 mV, < 5 mV and 200 mV, respectively, as shown in Figs. 21(a), 21(b) and ???. The experimental results are consistent the theory. The error is mainly caused by the existence of the equivalent series resistance (ESR) of the capacitor. The current ripples of LEDs driven by the VS boost converter, CS boost converter and CS boost converter with an extra capacitor are 24 mA, 240 mA and < 5 mV, respectively, as shown in Figs. 21(d), 21(e) and 21(f). The experimental results agree with the theory. For the CS buck converter, the inductor can be removed, reducing the size, weight and cost of the circuit. For the CS boost converter, a parallel capacitor should be connected to the output port to reduce the output

TABLE V
MEASURED OUTPUT RIPPLES OF VS AND CS CONVERTERS ($I_o = 600$ mA)

	VS buck conv.	CS buck conv.	CS buck conv. without L	VS boost conv.	CS boost conv.	CS boost conv. with extra C_o
Ripple	50 mV	very small	200 mV	24 mA	240 mA	very small
Percentage	0.16%	very small	0.64%	6.86%	68.6%	very small

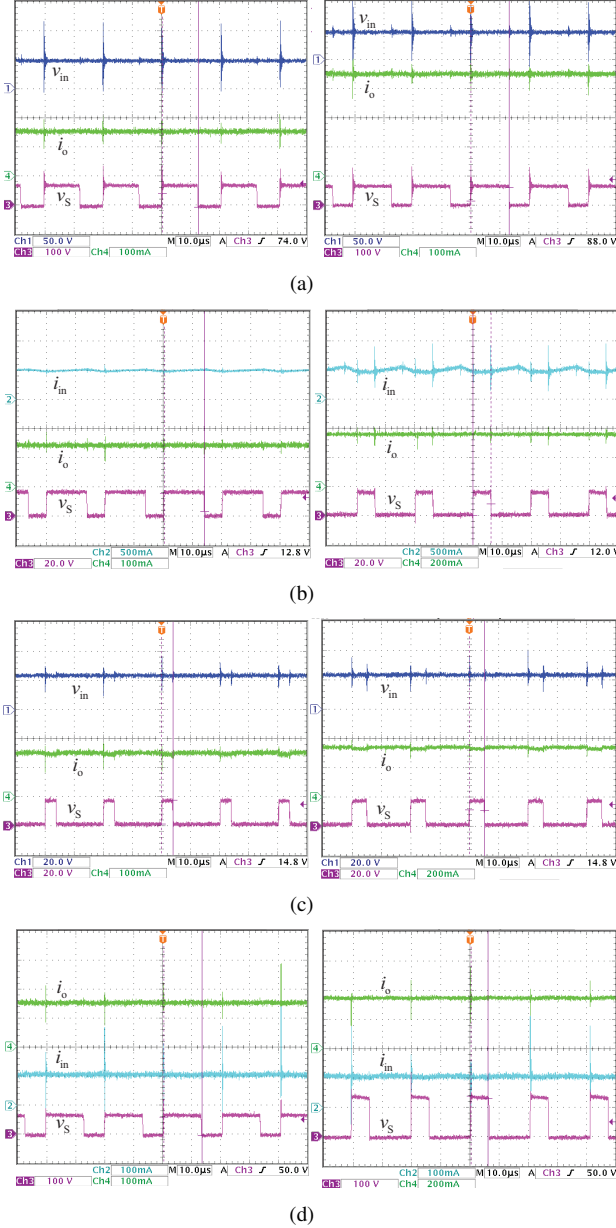


Fig. 22. Practical range of duty cycle. (a) VS buck converter $I_o = 150$ – 350 mA; (b) CS buck converter $I_o = 150$ – 350 mA; (c) VS boost converter $I_o = 150$ – 350 mA; (d) CS boost converter $I_o = 150$ – 350 mA.

current ripple. The measured ripple magnitudes are given in Table V.

Experimental waveforms for the range of duty cycle are shown in Fig. 22. The figures show the measured maximal and minimum duty cycle, D_{max} and D_{min} .

The measured D_{min} and D_{max} are consistent with theoret-

TABLE VI
MEASURED DUTY CYCLE ($I_o = 150$ – 350 mA)

	VS buck	CS buck	VS boost	CS boost
D_{max}	0.660	0.695	0.254	0.660
D_{min}	0.610	0.310	0.184	0.290
D_{span}	0.050	0.385	0.070	0.370

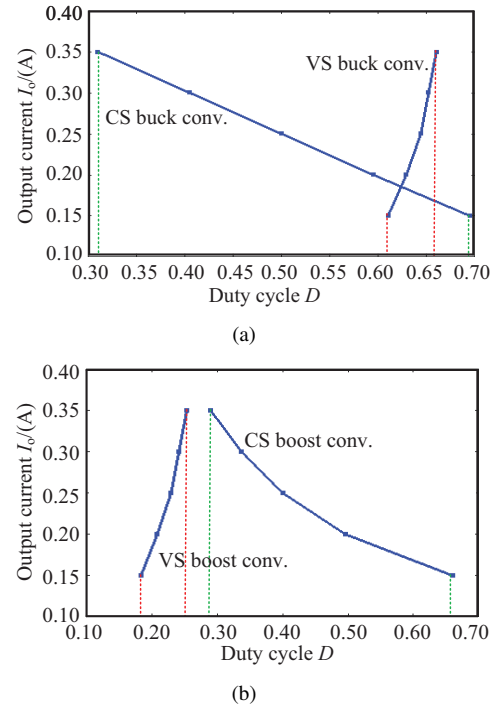


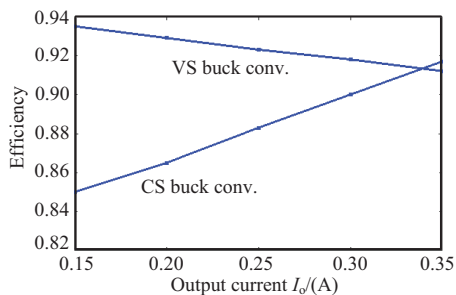
Fig. 23. Measured output current versus duty cycle. (a) VS and CS buck converters; (b) VS and CS boost converters.

ical results. The errors in VS converters are due to the device characteristic of the LED load, i.e., v - i characteristic, since the VS converter regulates the current through the LED's v - i curve. However, the CS converter regulates the current directly via the duty cycle. From the measured results, CS converters can control the output current using a wider range of duty cycle compared to VS converters. The results are given in Table VI.

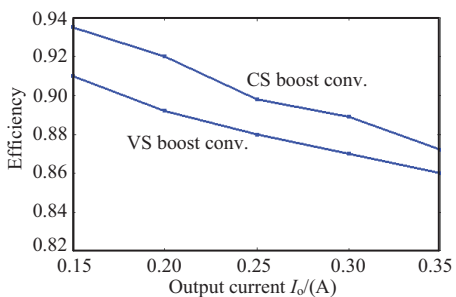
According to the measured output current and duty cycle, we can derive the relationship between output current and duty cycle, as shown in Fig. 23, from which we can find the practical values of S and N , as tabulated in Table VII. From the measured parameters, the CS converters have smaller S than VS converters. Notable error in S can be found in VS converters because of the device characteristic of the LED

TABLE VII
MEASURED PARAMETERS

	VS buck	CS buck	VS boost	CS boost
S_{\max}	6.25	0.53	4.17	1.06
S_{\min}	2.63	0.50	2.00	0.30
W	0.0125	0.0963	0.0175	0.0925
ΔW	0.0010	0.0004	0.0012	0.0096
N	0.0800	0.0042	0.0686	0.1038



(a)



(b)

Fig. 24. Comparison of the efficiency. (a) VS and CS buck converters; (b) VS and CS boost converters.

load. The CS buck converter has smaller N than the VS buck converter. However, the CS boost converter has bigger N than the VS boost converter.

The efficiencies, for comparison purposes, are plotted in Fig. 24. Compared with the VS buck converter, the CS buck converter has a lower efficiency because the MOSFET always conducts the input current which is higher than the output current. Compared with the VS boost converter, the CS boost converter has a higher efficiency.

Experimental waveforms for the two-stage driver are shown in Fig. 25. The input voltage in Fig. 25(a) is 48 V, which is larger than V_o . The measured duty cycle D_1 is 0.47, D_2 is 0.30, $D_1 + D_2 < 1$, consistent with theory. The input voltage in Fig. 25(b) is 26 V, which is smaller than V_o . The measured duty cycle D_1 is 0.87, D_2 is 0.30, $D_1 + D_2 > 1$, again consistent with the theory.

VI. CONCLUSION

In this paper, we examine the driving circuit requirement for LED loads. Our starting point is the LED characteristic and basic circuit theory. We highlight the importance of consideration of the termination type and the corresponding choice of converter type. Specifically we introduce the mostly

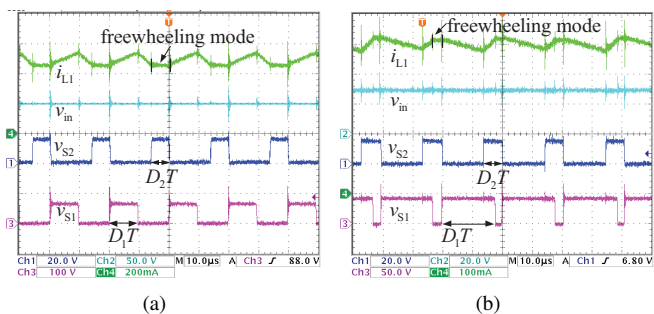


Fig. 25. Two-stage driver using VS buck converter cascading CS buck converter. (a) $V_{in} = 48$ V; (b) $V_{in} = 26$ V.

unknown current-source based converters which can be derived via the application of duality principle and compare these converters with the conventional and mostly known voltage-based converters. We focus on comparison of the key performance areas in relation to LED lighting applications. We emphasize that proper application of circuit concepts would form the basis of design of effective driving circuits for LED applications. Analytical and experimental details are provided in this paper.

REFERENCES

- [1] S. Li, S. C. Tan, C. K. Lee, E. Waffenschmidt, S. Y. R. Hui, and C. K. Tse, "A survey, classification, and critical review of light-emitting diode drivers," *IEEE Transactions on Power Electronics*, vol. 31, no. 2, pp. 1503–1516, 2016.
- [2] X. Qu, S. C. Wong, and C. K. Tse, "An improved lclc current-source-output multistring led driver with capacitive current balancing," *IEEE Transactions on Power Electronics*, vol. 30, no. 10, pp. 5783–5791, 2015.
- [3] M. H. Crawford, "Leds for solid-state lighting: performance challenges and recent advances," *IEEE Journal of Selected Topics in Quantum Electronics*, vol. 15, no. 4, pp. 1028–1040, 2009.
- [4] X. Qu, S. C. Wong, and C. K. Tse, "Noncascading structure for electronic ballast design for multiple led lamps with independent brightness control," *IEEE transactions on Power Electronics*, vol. 25, no. 2, pp. 331–340, 2010.
- [5] W. K. Lun, K. Loo, S. C. Tan, Y. Lai, and C. K. Tse, "Bilevel current driving technique for leds," *IEEE Transactions on Power Electronics*, vol. 24, no. 12, pp. 2920–2932, 2009.
- [6] H. Valipour, G. Rezaadeh, and M. R. Zolghadri, "Flicker-free electrolytic capacitor-less universal input offline led driver with pfc," *IEEE Transactions on Power Electronics*, vol. 31, no. 9, pp. 6553–6561, 2016.
- [7] S. Y. R. Hui, S. N. Li, X. H. Tao, W. Chen, and W. Ng, "A novel passive offline led driver with long lifetime," *IEEE Transactions on Power Electronics*, vol. 25, no. 10, pp. 2665–2672, 2010.
- [8] H. Kanchev, D. Lu, F. Colas, V. Lazarov, and B. Francois, "Energy management and operational planning of a microgrid with a pv-based active generator for smart grid applications," *IEEE transactions on industrial electronics*, vol. 58, no. 10, pp. 4583–4592, 2011.
- [9] J. Leppäaho and T. Suntio, "Dynamic characteristics of current-fed superbuck converter," *IEEE Transactions on Power Electronics*, vol. 26, no. 1, pp. 200–209, 2011.
- [10] D. Shmilovitz and S. Singer, "A switched mode converter suitable for superconductive magnetic energy storage (smes) systems," in *Applied Power Electronics Conference and Exposition, 2002. APEC 2002. Seventeenth Annual IEEE*, vol. 2, pp. 630–634, IEEE, 2002.
- [11] A. Andreičiks, I. Steiks, and O. Krievs, "Design of efficient current fed dc/dc converter for fuel cell applications," in *2011 IEEE International Symposium on Industrial Electronics*, pp. 206–210, IEEE, 2011.
- [12] X. Qu, S. C. Wong, and C. K. Tse, "Resonance-assisted buck converter for offline driving of power led replacement lamps," *IEEE Transactions on Power Electronics*, vol. 26, no. 2, pp. 532–540, 2011.

- [13] S. M. Chen, T. J. Liang, L. S. Yang, and J. F. Chen, "A boost converter with capacitor multiplier and coupled inductor for ac module applications," *IEEE transactions on Industrial electronics*, vol. 60, no. 4, pp. 1503–1511, 2013.
- [14] C. Qiao and K. M. Smedley, "A topology survey of single-stage power factor corrector with a boost type input-current-shaper," *IEEE Transactions on Power Electronics*, vol. 16, no. 3, pp. 360–368, 2001.
- [15] T. J. Liang, S. M. Chen, L. S. Yang, J. F. Chen, and A. Ioinovici, "A single switch boost-flyback dc-dc converter integrated with switched-capacitor cell," in *Power Electronics and ECCE Asia (ICPE & ECCE), 2011 IEEE 8th International Conference on*, pp. 2782–2787, IEEE, 2011.
- [16] N. M. Mapula and W. R. Liou, "Integrated multi-channel constant current led driver with pwm boost converter design in 0.35 μ m process," in *TENCON 2012-2012 IEEE Region 10 Conference*, pp. 1–6, IEEE, 2012.
- [17] J. Zhang, J. Wang, and X. Wu, "A capacitor-isolated led driver with inherent current balance capability," *IEEE Transactions on Industrial Electronics*, vol. 59, no. 4, pp. 1708–1716, 2012.
- [18] X. Wu, Z. Wang, and J. Zhang, "Design considerations for dual-output quasi-resonant flyback led driver with current-sharing transformer," *IEEE Transactions on Power Electronics*, vol. 28, no. 10, pp. 4820–4830, 2013.
- [19] D. Liu, A. Hu, G. Wang, and W. Hu, "Current sharing schemes for multiphase interleaved dc/dc converter with fpga implementation," in *Electrical and Control Engineering (ICECE), 2010 International Conference on*, pp. 3512–3515, IEEE, 2010.
- [20] C. K. Tse, *Linear Circuit Analysis*. Addison-Wesley, 1998.
- [21] R. Rabinovici and B. Kaplan, "Novel dc-dc convertor schemes obtained through duality principle and topological considerations," *Electronics Letters*, vol. 21, no. 27, pp. 1948–1950, 1991.
- [22] H. Martínez-García and A. Saberkeri, "Linear-assisted dc/dc regulator-based current source for led drivers," *Electronics Letters*, vol. 52, no. 6, pp. 437–439, 2016.
- [23] O. Tetervonok and I. Galkin, "Assessment of switch mode current sources for current fed led drivers," in *Doctoral Conference on Computing, Electrical and Industrial Systems*, pp. 551–558, Springer, 2014.
- [24] X. Liu, J. Xu, Q. Yang, and D. Xu, "High-efficiency multi-string led driver based on constant current bus with time-multiplexing control," *Electronics Letters*, vol. 52, no. 9, pp. 746–748, 2016.
- [25] I. Galkin, O. Tetervonok, and I. Milashevski, "Comparative study of steady-state performance of voltage and current fed dimmable led drivers," in *Compatibility and Power Electronics (CPE), 2013 8th International Conference on*, pp. 292–297, IEEE, 2013.
- [26] S. Li, Y. Guo, S. C. Tan, and S. Y. R. Hui, "An off-line single-inductor multiple-outputs led driver with high dimming precision and full dimming range," *IEEE Transactions on Power Electronics*, 2016.
- [27] B. Lehman and A. J. Wilkins, "Designing to mitigate effects of flicker in led lighting: Reducing risks to health and safety," *IEEE Power Electronics Magazine*, vol. 1, no. 3, pp. 18–26, 2014.
- [28] I. Galkin, I. Milashevski, and O. Teteryonok, "Comparative study of steady-state performance of led drivers at different modulation techniques," in *2011 7th International Conference-Workshop Compatibility and Power Electronics (CPE)*, pp. 382–387, IEEE, 2011.
- [29] C. K. Tse, Y. M. Lai, R. J. Xie, and M. H. L. Chow, "Application of duality principle to synthesis of single-stage power-factor-correction voltage regulators," *International Journal of Circuit Theory and Applications*, vol. 31, no. 6, pp. 555–570, 2003.